BBA - Molecular and Cell Biology of Lipids 1871 (2026) 159731

Contents lists available at ScienceDirect

BBA - Molecular and Cell Biology of Lipids

journal homepage: www.elsevier.com/locate/bbalip

Surfactant nebulization in severe COVID-19: Tracheal aspirate phospholipid turnover and metabolism

Anthony D. Postle [a,b,c,*], Howard W. Clark [d,f], James Fink [e], Jens Madsen [d], Grielof Koster [c], Madhuriben Panchal [c], Lewis Matthews [c], Lee Berry [c], Ratko Djukanovic [c], David Brealey [g], Michael P.W. Grocott [a,b,c], Ahilanandan Dushianthan [b,c]

[a] Clinical and Experimental Sciences, Sir Henry Wellcome Laboratories, Faculty of Medicine, University of Southampton, Southampton, SO16 6YD, UK
[b] Intergrative Physiology and Critical Illness Group, Faculty of Medicine, University of Southampton, SO16 6YD, UK
[c] National Institute for Health Research (NIHR) Southampton Biomedical Research Centre and Critical Care/Anaesthesia and Perioperative Medicine Research Unit, University Hospital Southampton National Health System Foundation Trust, Southampton, SO16 6YD, UK
[d] EGA Institute for Women's Health, Faculty of Population Health Sciences, University College London Hospital, Room 343, Medical School Building, 74, Huntley Street, London, WC1E 6AU, UK
[e] Aerogen Pharma Corporation, 1660 S. Amphlett Blvd, Suite 360, San Mateo, CA, 94402, USA
[f] NIHR University College London Hospital Biomedical Research Centre, Infection and Immunity Theme, 149 Tottenham Court Road, London, W1T 7DN, UK
[g] Division of Critical Care and NIHR University College London Hospitals Biomedical Research Centre, University College Hospitals London, 235 Euston Road, London, NW1 2BU, UK

ARTICLE INFO

Keywords:
COVID-19
Acute respiratory distress syndrome
Surfactant phospholipid
Turnover
Metabolism

ABSTRACT

COV-SARS-2 targets alveolar type II cells. As these cells synthesise lung surfactant, we hypothesised that surfactant dysfunction may contribute to development of ARDS in COVID-19. Here we report turnover of surfactant delivered to patients ventilated for severe COVID-19 using a novel breath-synchronized nebulizer compared with a control group. Endogenous surfactant status, turnover and half-life of administered surfactant and tracheal aspirate (TA) phospholipid metabolism were analysed by lipidomic mass spectrometry. At enrolment shortly after intubation, TA analysis (n = 20) showed markedly reduced concentrations of surfactant phospholipids, consistent with surfactant depletion. In a dose-range study in 12 ventilated COVID-19 patients with ARDS, administered surfactant resulted mean 20-fold (range 6.4 and 60.3) excess over endogenous lipid, providing proof of concept for effective nebulization, with a very rapid turnover (median half-life 7.8, range 0.4 to 20.8 h). Neither the rate of endogenous TA phosphatidylcholine (PC) synthesis nor the composition of newly synthesised PC, determined by incorporation of *methyl*-D_9-choline, were significantly altered by exogenous surfactant nebulization. An inverse correlation between the fractional synthesis of dipalmitoyl phosphatidylcholine and inflammatory status suggested that a significant portion of endogenous TA phospholipid was derived from non-surfactant sources. This analysis is the first direct demonstration of surfactant deficiency in COVID-19; while exogenous surfactant can correct this deficiency, its rapid turnover suggests that prolonged treatment with surfactant will be needed.

1. Introduction

The SARS-CoV-2 virus targets the ACE-2 receptor on type II alveolar epithelial (ATII) cells, resulting in extensive cell damage and depletion in cell numbers [1–3]. An important function of the ATII cell is synthesis and secretion of lung surfactant, the lipid:protein complex responsible for preventing alveolar collapse by reducing surface tension forces in the lungs [4]. Surfactant dysfunction is central to the pathogenesis of Acute Respiratory Distress Syndrome [ARDS]) due to a combination of reduced concentration and inhibition by oedema proteins [5]. Severe SARS-CoV-2 infection is associated with a clinical picture of ARDS, characterised by poor alveolar compliance with diffuse premature alveolar collapse and flooding with oedema fluid. Surfactant deficiency has also been suggested to play a role in the progression to ARDS in

* Corresponding author at: Clinical and Experimental Sciences, Sir Henry Wellcome Laboratories, Faculty of Medicine, University Hospital Southampton, Tremona Road, Southampton, SO16 6YD, UK.
E-mail address: adp@soton.ac.uk (A.D. Postle).

https://doi.org/10.1016/j.bbalip.2026.159731
Received 12 October 2025; Received in revised form 16 January 2026; Accepted 6 February 2026
Available online 10 February 2026

COVID-19, [6–8]. While small observational or retrospective studies have suggested some benefit, our previous report of the clinical outcomes of this randomised controlled trial of therapeutic surfactant administration in COVID-19 patients showed no significant efficiency in mitigating ARDS severity [9]. While this is likely related to number of reasons, there is a critical need to establish strategies to optimise dose concentration, dose frequency and duration and mode of delivery. To date, there are no reports characterising the metabolism in vivo of both endogenous and exogenous surfactant in COVID-19.

Although previous trials of surfactant administration in ARDS have proved unsuccessful, there are good reasons to suggest surfactant therapy may be beneficial to patients with severe COVID-19 [10]. Previous ARDS trials recruited heterogeneous cohorts of patients with both alveolar and systemic underlying aetiologies that are likely to have different impacts on surfactant metabolism and function. Patients infected with SARS-CoV-2 are a more homogeneous population, with viral pneumonia causing extensive direct damage to the alveolar epithelium, leading to the need for invasive ventilator support. Consequently, we reasoned that surfactant therapy might be more effective in a patient group with common aetiology. In addition, previous trials have administered surfactant either as bolus doses, with the added problems caused by large liquid volumes in patients with compromised lungs or by nebulization [11]. While devices for continuous nebulization have proved inefficient for surfactant delivery [12], novel breath-synchronized nebulizers have the potential for more efficient delivery. Consequently, in this pilot study, we evaluated the effectiveness of a prototype breath-synchronized vibrating mesh nebulizer to deliver exogenous surfactant to patients ventilated for severe COVID-19 infection [13,14]. The aim of this study was to document the impact of surfactant nebulization on endogenous and exogenous phospholipid metabolism in the lungs of patients ventilated for severe COVID-19 infection. We report here our findings on surfactant amounts delivered, turnover and half-life. In addition, we investigated the initial surfactant status of patients and the effects of exogenous surfactant on endogenous phospholipid metabolism.

2. Methods

2.1. Patient population

Eligible participants were aged >18 years old, SARS-CoV-2 confirmed requiring invasive mechanical ventilation for moderate to severe hypoxic respiratory failure (9). All participants were mechanically ventilated and enrolled within 24 h of endotracheal intubation and randomised to 3:2 for surfactant and control arms. The study protocol was approved by the Health Research Authority (REC reference: 20/NE/0149 and IRAS: 282498) and MHRA (EudraCT number: 2020–001886-35) [14]. We compared COVID-19 patients with historic data from healthy control patients (REC: 11/SC/0185 and IRAS: 76100) [15]. The patient characteristics at recruitment have been published previously [9] and are summarised in Table 1.

2.2. Methyl-D_9-choline infusion

Trimethyl-D_9-choline chloride (DLM-549-1) (CK Isotopes Newtown Unthank, UK) was sterile formulated by NOVA Laboratories Limited (Leicester, UK) in water at 1 mg/ml. All patients in the treated groups were infused 3 h before surfactant nebulisation with 3 mg/kg body weight of *methyl*-D_9-choline over 3-h though an existing peripheral or central catheter or at an equivalent time for patients in the control group. This methodology has been successfully used previously in healthy volunteers [15], preterm infants [16] and ARDS patients [17].

2.3. Nebulization of surfactant

Surfactant was nebulized using a breath-synchronized vibrating mesh nebulizer (Aerogen Pharma) [13]. Patients randomised to surfactant received a natural bovine surfactant preparation, supplied as 108 mg/vials of a lyophilised powder (Alveofact®, Lyomark GmbH, Germany), widely used in preterm neonates [18,19], reconstituted to 45 mg/ml in buffer supplied in a pre-filled syringe. There were two protocols for surfactant nebulization. Six patients in protocol 1 received three doses of 1080 mg of Alveofact®, Lyomark GmbH, Germany) at $T = 0$, 8 and 24 h with four patients acting as controls, receiving standard clinical care. An interim analysis of Alveofact turnover in patients in protocol 1 indicated a very rapid half-life of ~7.6 h (range 1.8–20.8 h) [20]. Consequently, the protocol for surfactant nebulixation was modified to give the same total dose of Alveofact at six instead of three time points. Six patients in protocol 2 received a randomised dosing regimen of six nebulizations of a reduced dose of 540 mg Alveofact at extended times $T = 0$, 12, 24, 36, 48 and 72 h.

Table 1
Patient details at study recruitment. Data is presented as mean ± s.d., n (%) or median ± IQR, with no significant differences between groups.

Baseline characteristics	All patients (n = 20)	Control group (n = 8)	Surfactant group (n = 12)
Age-yrs	55.9 ± 12.7	56.5 ± 11.4	55.5 ± 14.0
Female gender	8 (40%)	3 (38%)	5 (42%)
Ethnicity			
White	16 (80%)	7 (88%)	9 (75%)
Mixed	2 (10%)	0 (0%)	2 (17%)
Asian	2 (10%)	1 (13%)	1 (8%)
Body mass index (kg/m^2)	32.3 (28.0–38.8)	30.8 (27.8–42.0)	33.5 (28.0–38.8)
Neutrophil/lymphocyte ratio	12.3 (6.8–23.4)	9.5 (6.4–13.1)	17.0 (10.2–24.5)
Duration hospitalization before study recruitment, (hours)	107 (69–221)	194 (126–244)	93 (64–125)

2.4. Closed tracheal aspirate sample collection, processing and storage

TA samples from all patients were collected following 10-50 ml of 0.9% saline instillation by closed in-line tracheal suction at 0, 8, 16, 24, 48 and 72 h after *methyl*-D_9choline infusion. Samples at $T = 0$ h, $T = 8$ h and $T = 24$ h were taken in advance of surfactant nebulization at those times. TA samples (5-10 ml) were processed in a containment level 2 microbiological safety cabinet and filtered through a 100 μm mesh filter before centrifugation at 400xgx10 minutes at 4 °C. A supernatant aliquot (800 μl) was added to 2 m ice cold methanol and 10 μl butylated hydroxytoluene antioxidant (20 g/L), capped and stored at −80 °C until further processing. Methanol was added as this early processing stage to inactivate the virus. The schedule of *methyl*-D_9-choline infusion, Alveofact nebulisation and TA and blood sampling are summarised in Fig. 1.

2.5. Phospholipid extraction

Total lipids from TA samples were extracted using dichloromethane and methanol as described previously [15] after adding 15 μl of an internal standard mixture (15 μl) (SPLASH® LIPIDOMIX®, Supplementary Table 1, Avanti Polar Lipids, Alabaster, USA).

2.6. ESI/MS-MS analysis

Dried lipid extracts were re-suspended in a mixture of methanol-butanol-water-concentrated NH_4OH (6:2:1.6:0.4 *v*/v) and injected directly into the electrospray ionisation interface of a Xevo TQ mass spectrometer (Waters Corporation, UK) (ESI-MS/MS) at 5 μl/min. MS/MS precursor ion scans identified unlabelled phosphatidylcholine (PC), lysophosphatidylcholine (LPC) and sphingomyelin (SM) (m/z 184^+),

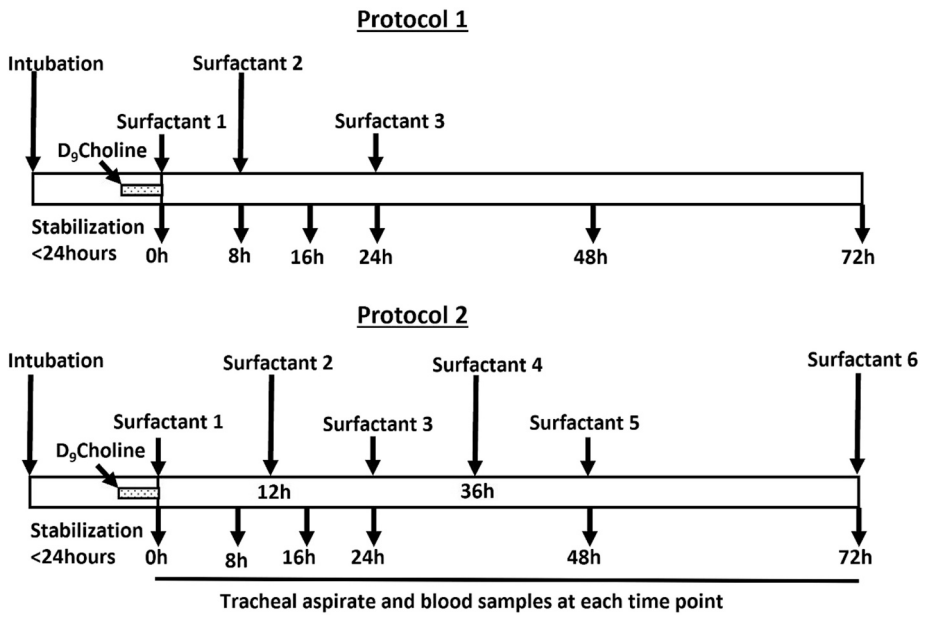

Fig. 1. Summary of study protocols. Treated patients in protocol 1 were nebulised with three doses of 1080 mg Alveofact at $T = 0$, 8 and 24 h. Treated patients in protocol 2 were nebulized with six doses of 540 mg Alveofact at T = 0, 12, 24, 36, 48 and 72 h. All patients were infused with 3.0 mg/kg *methyl*-D_9choline over 3 h before the start of nebulisztion or at the equivalent time for control patients. TA and blood samples were taken at T = 0, 8, 16, 24, 48 and 72 h, with those at $T = 24$, 48 and 72 h taken before Alveofact nebulisation depending on the protocol.

phosphatidylglycerol (PG) (m/z 153^-), phosphatidylinositol (PI) (m/z 241^-) and *methyl*-D_9 labelled PC, LPC and SM (m/z 193^+). Neutral loss scans identified phosphatidylinositol (PE) (m/z 141^+) and phosphatidylserine (m/z 87^-).

2.7. Data extraction, analysis and statistics

Mass spectrometry data exported from MassLynx 4.1 (Waters Corporation, UK) was processed by an in-house programme [16,17].

Percentage compositions, concentrations calculated relative to the internal standards and label enrichments were then analysed in GraphPad Prism 10.0 and presented as means and either standard deviation or standard error. Significance was determined by an unpaired two tailed *t*-test, Mann-Whitney U or two-way ANOVA tests where appropriate. Historical healthy volunteer data from nine study participants [15] was used for baseline comparison of TA PC compositions at recruitment to the study.

2.7.1. Kinetic modelling of supplemented surfactant

Kinetic optimization of exogenous surfactant turnover for patients in protocol 1was estimated from the difference in fractional concentration of SM16:0 between Alveofact and endogenous tracheal aspirate samples. As Alveofact sphingomyelin fractional concentration was tenfold to fifteen-fold lower than that of tracheal aspirates at $T = 0$ h, sphingomyelin was used as a proxy marker for endogenous lipid in the surfactant-treated patients. SM16:0 was chosen for this calculation as it could be reliably quantified in all samples even at very low concentrations. Optimization was achieved by minimizing the sum of the square of the difference between the square root of 1/SM16:0(%) measured at each time point and the calculated value for that time point. The calculations for each time point are shown in the equations below, where C_{tX} is the calculated value at time X, A_0 is the added amount of Alveofact at each administration, k is the exponential decay constant and Bg is the concentration of SM16:0 in Alveofact, expressed as percentage of total phospholipid. M_{t0} is the measured concentration of SM16:0 in tracheal aspirates at $T = 0$ h, expressed as percentage of total phospholipid. Each of the parameters A_0, k and Bg were optimized for each patient by an iterative process, set out in Supplementary Table 2.

$$Ct0 = Mt0$$

$$Ct8 = \frac{1}{\frac{1}{A0*e^{(k*8)}} + Bg} + Mt0$$

$$Ct16 = \frac{1}{\frac{1}{A0*\left(e^{(-k*16)}+e^{(-k*8)}\right)} + Bg} + Mt0$$

$$Ct24 = \frac{1}{\frac{1}{A0*\left(e^{(-k*24)}+e^{(-k*16)}\right)} + Bg} + Mt0$$

$$Ct48 = \frac{1}{\frac{1}{A0*\left(e^{(-k*48)}+e^{(-k*40)}+e^{(-k*24)}\right)} + Bg} + Mt0$$

$$Ct72 = \frac{1}{\frac{1}{A0*\left(e^{(-k*72)}+e^{(-k*64)}+e^{(-k*48)}\right)} + Bg} + Mt0$$

The proportion of endogenous PC in aspirates from surfactant-treated patients was calculated from the equation:

$$x = \frac{Mt - Alv}{M0 - Alv}$$

where X = fraction of endogenous lipid at time t, M0 = %SM16:0 at $T = 0$, Mt. = %SM16:0 at time t and Alv = %SM16:0 in Alveofact.

2.7.2. Data availability

Source data is available from the authors on request.

3. Results

3.1. Tracheal aspirate phospholipid compositions

Phospholipid analysis of baseline tracheal aspirates indicated that pulmonary surfactant was significantly compromised in patients ventilated for COVID-19 infection. Percentage phospholipid class composition was comparable between all study groups and significantly different

from that of the administered Alveofact surfactant (Table 2). PC and PG, typically enriched in surfactant, were both lower in all study groups than in Alveofact and healthy control volunteers [15], with corresponding increased concentration of phospholipids characteristic of cellular membranes, such as PS and SM. The consistently high contribution of PS to total phospholipid was striking and potentially important given its role in the clotting cascade [21]. The negative ionisation spectra from representative healthy control and COVID-19 patient shown in Fig. 2A and B respectively illustrate this difference, highlighting the dominance of PS over other acidic PL in the patient sample. There were no significant differences in the percentage phospholipid class composition between the three patient groups, while all were significantly different ($p < 0.01$) compared with administered Alveofact (Table 2). Absolute phospholipid concentrations were highly variable and were not significantly different between the three study groups (Table 2).

The tracheal aspirate phospholipid class composition approached that of administered Alveofact at $t = 8$ h to $t = 16$ h for patients in both protocol 1 (Fig. 2C) and protocol 2 (Fig. 2D), indicating that recovered phospholipid was essentially administered Alveofact at these time points. Maximal values for PC were 80.5 ± 3.8% and 80.0 ± 2.0% total phospholipid for patients in protocols 1 and 2 respectively. PC concentration declined slowly with time but remained significantly above baseline and control group vales at all time points, with no significant differences between the two surfactant protocol groups at any time. The changes to the minor PL classes, plotted without the PC data, are illustrated more clearly in Figs. 2 E and 2F for protocol 1 and 2 respectively. There were no significant changes to tracheal aspirate phospholipid class compositions between $T = 0$ h to $T = 72$ h in control patients (Fig. 2 G). Importantly for turnover calculations for patients in protocol 1, the fractional composition of SM remained constant over this period in the control patient group. By contrast, phospholipid composition at $T = 8$ h in tracheal aspirate samples from surfactant-treated patients changed substantially to resemble that of Alveofact. PG concentration increased from 3.7 ± 1.8 to a maximum of 13.3 ± 3.3% for patients in protocol 1 and from 5.7 ± 5.2% to 12.9 ± 7.4% for patients in protocol 2 and remained elevated throughout the study. Comparison between total PC and total PG for the treated groups suggests Alveofact PC and PG were metabolised at comparable rates. Concentrations of all other acidic phospholipid classes declined after Alveofact nebulization but recovered substantially with time.

3.2. Exogenous surfactant turnover

Phospholipid concentrations of tracheal aspirate samples varied widely, especially in surfactant-treated patients due to a combination of factors, including variable recovery of instilled saline and the viscous mucoid state of the samples, which made filtration of the aqueous fluid phase difficult. Consequently, it was not possible to calculate exogenous surfactant turnover from absolute lipid concentration. Instead, the concentration of exogenous surfactant was determined relative to that of endogenous lipid in tracheal aspirate samples. This calculation was dependent on the compositional differences between administered Alveofact and endogenous lipid (Table 2) and the demonstration of no significant PL class change in the control patient group over the duration of the study. The consequent assumption that concentration and composition of endogenous lipid in the Alveofact patient groups also did not change substantially over the 72-h study period was supported by the increases to acidic PL classes at $T = 72$ h shown in Fig. 2E and F.

As the fractional concentration of major SM species SM16:0 in Alveofact was approximately tenfold-fold lower than that of tracheal aspirates at $T = 0$ h, this molecular species was used as a proxy marker for endogenous lipid in the surfactant-treated patients. An index of Alveofact concentration relative to endogenous tracheal aspirate phospholipid was then calculated for patients in protocol 1 as the reciprocal of the percentage concentration of SM16:0. This index was calculated for each patient; it was maximal for all treated patients between $T = 8$ and $T = 16$ h and returned to near baseline values by T = 72 h (Fig. 3A). It is important to highlight that this index is not a direct measure of the relative concentration of Alveofact, as the maximal value is determined by the concentration of SM in Alveofact. It does, however, illustrate the variation in Alveofact metabolism and demonstrates a rapid catabolism of administered surfactant. Kinetic models of these data for patients in protocol 1 were constructed by superimposing three first order exponential decay curves at $T = 0$ h, T = 8 h and $T = 24$ h, described in detail in the methods section, and maximal values and exponential constants were determined empirically by an iterative process, shown schematically in Fig. 3B. This then enabled estimation of Alveofact half-life, turnover and relative concentration which are summarised in Fig. 3 and Table 3 with derived kinetic parameters in Supplementary Table 3. Additionally, average half-life values, calculated from the reciprocals of the mean %SM16:0 concentrations (Fig. 3C) show reasonable agreement for both measured and modelled data.

Because the kinetic modelling required at least three sampling times after the last Alveofact nebulization, it could not be applied to patients in protocol 2 where the last sampling time was just before the last nebulization at $T = 72$ h. Instead, the calculated half-lives of individual patients in protocol 1 were correlated with the decrease of their 1/SM16:0 values between $T = 16$ and $T = 24$ h (Fig. 3D). Half-lives for patients in protocol 2 were then estimated from the decreases in their 1/SM16:0 values using this derived equation and are also shown in Table 2. While this indirect approach inevitably creates a greater uncertainty, these estimated half-lives suggest nebulized Alveofact catabolism was equally rapid in these cohorts. The median estimated Alveofact half-life for all twelve treated patients was 7.8, range 0.4–20.7 h. We then investigated

Table 2
Phospholipid class composition at baseline t = 0 h for all groups of COVID-19 patients in comparison to the Alveofact composition, expressed as percentage of total phospholipid (mean ± SEM) or concentration (median, IQR). There were no significant differences between the patient cohort phospholipid percentage compositions. All patient compositions were significantly different from Alveofact. (*p < 0.001, two-way Annova).

Phospholipid class	Control group (n = 8)	Alveofact group protocol 1 (n = 6)	Alveofact group protocol 2 (n = 6)	Alveofact suspension (n = 4)
Percentage				
Phosphatidylcholine (%)	47.8 ± 12.8	44.2 ± 11.7	45.2 ± 7.8	*81.4 ± 0.6
Phosphatidylglycerol (%)	3.7 ± 2.1	3.7 ± 1.8	5.7 ± 5.2	*10.3 ± 1.5
Phosphatidylethanolamine (%)	12.0 ± 4.2	15.6 ± 8.7	10.0 ± 2.7	*4.0 ± 0.4
Phosphatidylinositol (%)	4.0 ± 0.5	3.9 ± 1.2	3.7 ± 1.2	*2.3 ± 0.5
Phosphatidylserine (%)	21.8 ± 8.4	21.3 ± 7.7	26.2 ± 0.8	*0.9 ± 0.5
Sphingomyelin (%)	10.7 ± 5.8	11.4 ± 3.1	9.3 ± 2.5	*1.2 ± 0.2
Concentration (nmoles/ml, median, IOR)				
Phosphatidylcholine	26.8, 11.3–54.4	11.2, 1.4–11.0	8.9, 4.7–14.3	
Phosphatidylglycerol	1.4, 0.9–4.0	0.9, 0.3–2.3	0.7, 2.5–3.0	
Phosphatidylethanolamine	4.6, 2.5–10.5	5.1, 1.8–6.6	1.6, 1.2–3.1	
Phosphatidylinositol	2.3, 1.0–3.9	1.0, 0.4–3.0	0.6, 0.3–1.6	
Phosphatidylserine	6.6, 5.2–24.1	6.3, 2.2–11.1	4.5, 2.2–10.0	
Sphingomyelin	3.2, 2.6–9.6	3.0, 1.3–6.5	1.7, 1.1–2.8	

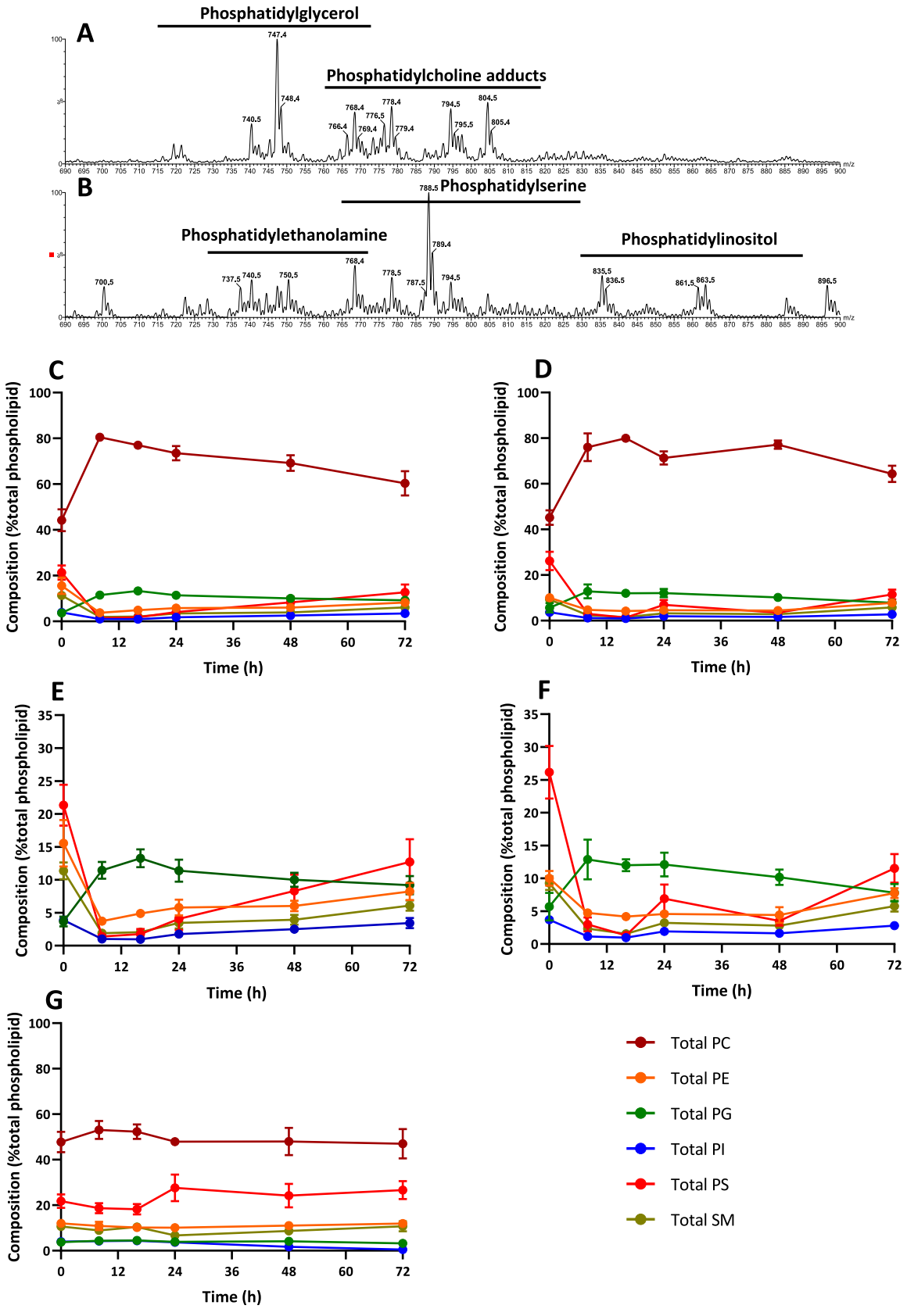

Fig. 2. Phospholipid composition in response to Alveofact nebulization Negative ionisation ESI-MS scans of lipid extracts of TA samples from a healthy control (**A**) and a patient with severe COVID-19 infection (**B**), demonstrating the increased abundance of PE, PS and PI and reduced PG in COVID-19. C. Phospholipid class compositions of patients in (C) the Alveofact group protocol 1 ($n = 6$), (**D**) Alveofact protocol 2 ($n = 6$). Panels **E** and **F** highlight the changes to the respective Alveofact cohorts to the minor phospholipids without PC. **G** Control group ($n = 8$). Results are means ± s.e.m.

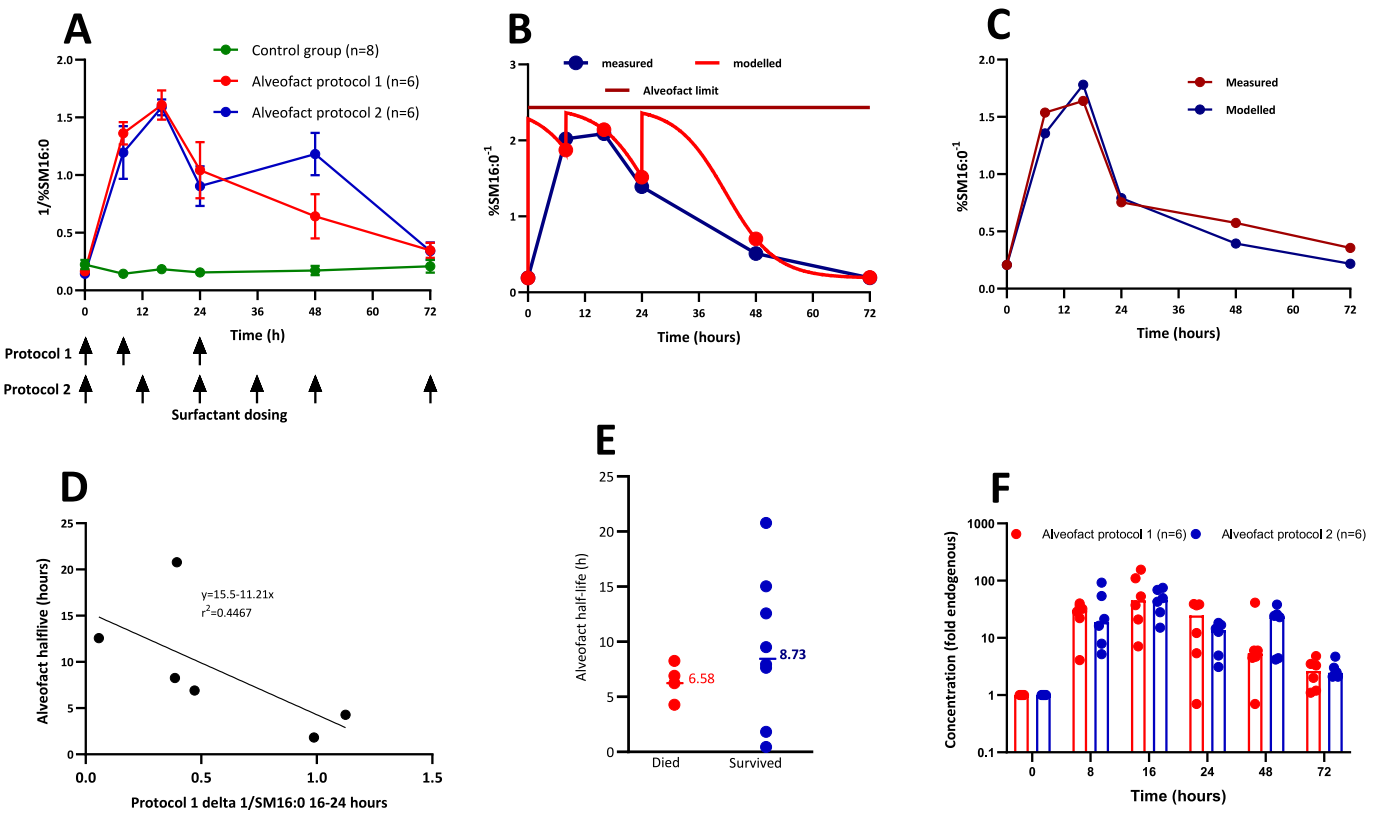

Fig. 3. Turnover of nebulized Alveofact in patients with COVID-19. A Reciprocal of SM16:0 percentage concentration in tracheal aspirate samples from Alveofact group protocol 1, Alveofact protocol 2 and control group; **B** Schematic of the modelling protocol for calculation of Alveofact kinetics in protocol 1. **C.** Comparison of measured and modelled profiles for patients in protocol 1. **D** Correlation for protocol 1 between calculated Alveofact half-life and the decrease of SM16:0 reciprocal between 16 and 24 h. **E** Calculated half-lives for all patients in the Alveofact cohorts. The median values were no different for patients who died (median 6.6 h, $n = 4$) and who survived for 28 days post ventilation (median 8.7 h, n = 8). **F** Concentration of tracheal aspirate Alveofact calculated relative to endogenous phospholipid for Alveofact protocol 1 & Alvofact protocol 2.

Table 3
Estimated half-lives of Alveofact. The half-life of patients in protocol 1 is derived from kinetic modelling data from three superimposed exponential decay curves. Alveofact half-lives for patients in protocol 2 were estimated by comparison withpatients in protocol 1 using the equation y = 15.5–11.21×, where y is Alveofact half-life and x is delta 1/SM16:0 between 16 and 24 h. Results are presented as medians and inter-quartile ranges.

	Alveofact half-life (h)	
	Protocol 1	Protocol 2
	20.7	6.2
	6.9	8.0
	8.2	7.7
	1.8	15.0
	12.6	9.5
	4.3	0.4
Cohort Medians (IQR)	**7.6 (3.6–14.6)**	**7.8 (4.8–10.9)**
Total Median (IQR)	**7.8 (4.7–11.8)**	

whether Alveofact turnover was more rapid in the patients who died before 8 days compared with those that survived, but there was no statistical difference (Fig. 3E).

The proportion of endogenous PC in aspirates from surfactant-treated patients was calculated from the equation $x = \frac{Mt - Alv}{M0 - Alv}$ as described in the methods. Fig. 2F shows the concentration of Alveofact at each time point (y), expressed as a multiple of the endogenous lipid concentration, given by the equation $y = \frac{1-x}{x}$. While it is important to recognise this is a relative concentration dependent on the unknown concentration of endogenous phospholipid, the results in Fig. 2F suggest that both nebulization protocols achieved comparable Alveofact concentrations in the lungs.

3.3. Phosphatidylcholine and sphingomyelin molecular species compositions

The baseline composition of selected molecular species of PC and SM are shown in Fig. 4A in comparison with values from healthy volunteers [15] and the Alveofact suspension. The fractional concentrations of dipalmitoylphosphatidylcholine (PC32:0), the major surface-active component of surfactant, in tracheal aspirate samples from COVID-19 patients was almost half that of comparable samples from healthy volunteers (24.9 ± 9.1 vs 45.3 ± 6.7%, $P < 0.001$). The percentage composition of PC and SM was identical between control and both Alveofact-treated cohorts, confirming comparable baseline compositions. Concentration of SM16:0, the most abundant SM species was significantly elevated in aspirates from patients (6.8 ± 2.8%) compared with healthy controls (1.8 ± 0.4%, $p < 0.001$) and Alveofact (0.7 ± 0.1%, $p < 0.001$). The volcano plots demonstrate elevated monounsaturated PC species in COVID-19 patients compared with Alveofact (Fig. 4B) but increased disaturated PC species in healthy volunteers compared with COVID-19 patients (Fig. 4C). Absolute concentrations of the selected species of PC and SM were highly variable and are summarised in Supplementary Table 4.

3.4. Phosphatidylcholine and sphingomyelin synthesis

In addition to rapid catabolism, depletion of endogenous surfactant may also be due to altered synthesis and secretion from ATII cells. PC synthesis was monitored in tracheal aspirates by the incorporation of

methyl-D_9-choline administered i.v. at $T = 0$ h, with incorporation being maximal between $T = 48$ h and $T = 72$ h for patients in the control group (Fig. 5A). This is consistent with our previous studies of surfactant PC synthesis in ARDS patients, which were based on analysis of small volume BAL samples [17]. As anticipated, the fractional *methyl*-D_9-choline incorporation into tracheal aspirate PC was substantially lower in Alveofact-treated patients as enrichment was calculated relative to total PC, which included that derived from Alveofact (Fig. 5A). We sought to correct this by using the relative concentration of endogenous tracheal aspirate PC derived from the turnover results presented in Fig. 3, based on the fractional concentration of SM16:0 (eq. 1 above). This correction substantially increased the apparent enrichment of *methyl*-D_9-choline in PC, such that enrichment at $T = 72$ h was not significantly different for both control and combined Alveofact-treated patients (Fig. 5B). This time point was selected for further comparisons as it provided the most reliable assessment of the specificity of PC synthesis in the Alveofact-treated patients. The enrichment of label in PC shown in Fig. 5 A and B does not take concentration into account, and total amounts of lipid synthesised can be very different over a range of concentrations even when fractional incorporation rates are equivalent. We wished, therefore, to determine the extent to which *methyl*-D_9-choline label incorporation into PC reflected endogenous surfactant synthesis. Consequently, we calculated the fractional composition of all *methyl*-D_9-choline-labelled PC species at $T = 72$ h, expressed as a percentage of the sum of total *methyl*-D_9-choline, which has the advantage of being independent of dilution with Alveofact. The use of this a surrogate marker was supported by the close correlation of the fractional compositions of unlabelled and labelled PC in the control group at 72 h (Supplementary Fig. 1, $R^2 = 0.87$, $p < 0.01$). There were no significant differences in this incorporation pattern at $T = 72$ h (Fig. 5C), suggesting that Alveofact administration did not alter the specificity of endogenous surfactant PC synthesis. Incorporation of *methyl*-D_9-choline into SM also increased with time for both groups of patients (Fig. 5D). However, the rate of label incorporation into SM was lower than for PC and was not

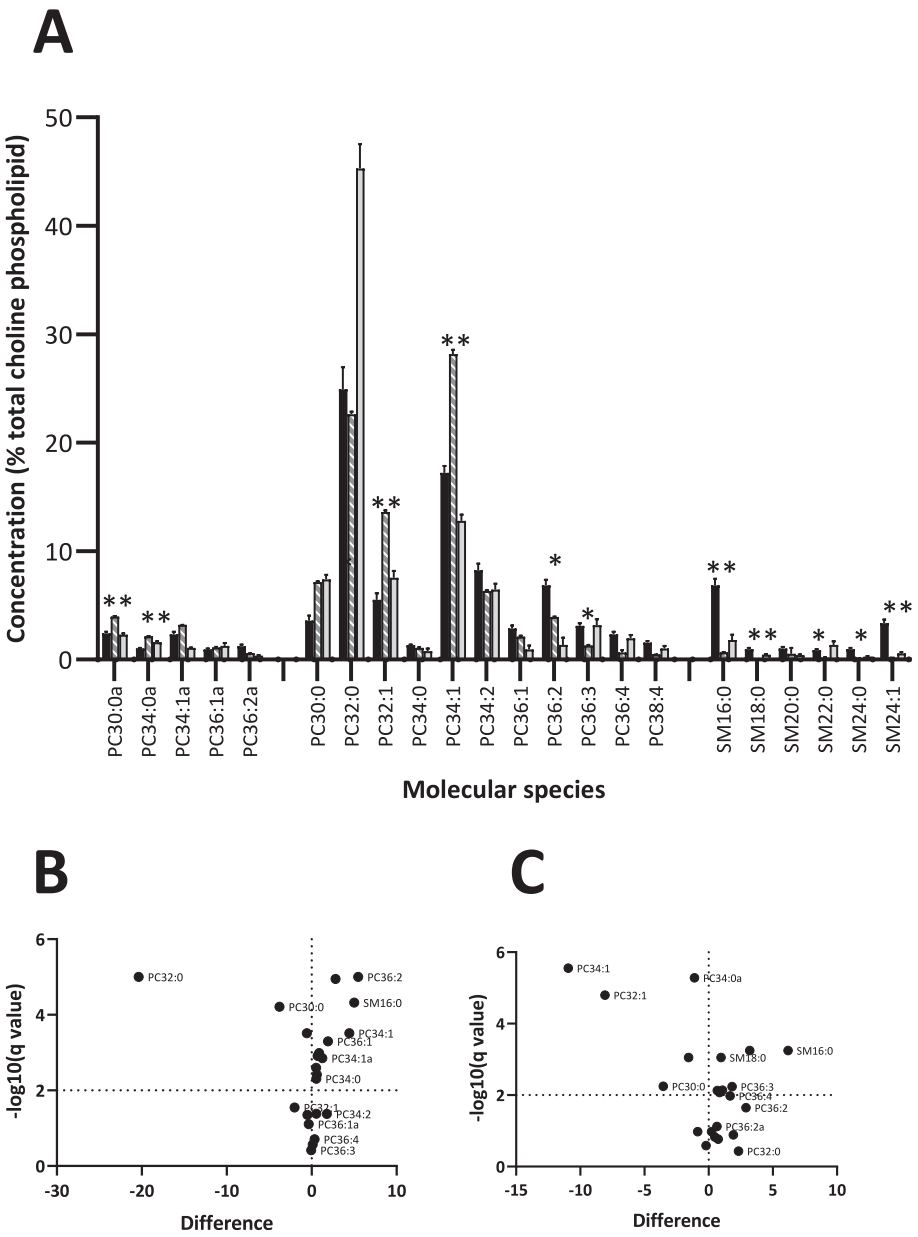

Fig. 4. Comparison of phosphatidylcholine and sphingomyelin molecular species. A COVID-19 patients at $t = 0$ h (solid bars, $n = 20$), Alveofact (hatched bars, n = 4), healthy control patients (grey bars, $n = 9$). Results are presented as means ± s.e.m., * $p < 0.01$, ** $p < 0.001$ for COVID-19 patients compared with Alveofact. Volcano plots for **B** COVID-19 patients compared with Alveofact; **C** COVID-19 patients compared with healthy volunteers.

significantly impacted by dilution with Alveofact, which has a low proportion of SM. *Methyl*-D_9-choline incorporation into SM from the surfactant-treated patients was not significantly different from that of control patients.

The specificity of aspirate PC synthesis at $T = 72$ h was not related to clinical status (P/F ratio, Supplementary Fig. 3) but further correlations suggested an association with inflammatory status. There was a positive correlation for all TA samples from control patients between concentrations of other PC species characteristic of surfactant (PC30:0 and PC32:1) (23, 24) and that of PC32:0, suggesting synchronous synthesis and secretion (Fig. 6A). However, concentration of the unsaturated species PC34:1 negatively correlated with PC32:0 (Fig. 6A) suggesting a possible different cellular origin from surfactant. This comparison could not be made for the treated group as PC composition was dominated by exogenous surfactant.

However, as the fractional composition of newly synthesised PC at $T = 72$ h reflected endogenous synthesis (Fig. 5C), this was used for comparison with inflammatory status. There was a strikingly different association for the patients who died within 28 days of ventilation of the fractional concentration of newly synthesised PC32:0 (% D_9PC32:0) at T = 72 h with the blood neutrophil:lymphocyte ratio at the same time point, as an indicator of overall inflammation (Fig. 6B). In agreement with other studies, the blood neutrophil:lymphocyte ratio at $T = 0$ h was significantly increased in the patients who died within 28 days of ventilation (26.8 ± 6.7 versus 11.6 ± 1.8, $p < 0.01$, mean ± sem, unpaired *t*-test) and also at $T = 72$ h (30.9 ± 6.5 versus 11.1 ± 1.5, $p < 0.001$) but was negatively correlated with % D_9PC32:0 at T = 72 h for patients who survived. This correlation was lost for the patients who died. There was no significant difference of the fractional synthesis of PC32:0 at T = 72 h between patients who died and those who survived.

There was little evidence for either enhanced phospholipase-mediated hydrolysis or lipid oxidation in these samples. LPC was <1% of total choline-containing lipids in TA samples at all time-points and did not increase in parallel with Alveofact catabolism (Supplementary Fig. 2). If phospholipase A_2 is involved in Alveofact hydrolysis, then the lysophospholipid products generated must be very rapidly further metabolised. Our results do not preclude activities of phospholipase C or D, as we did not measure diacylglycerol or phosphatiditic acid. While we did not conduct an-in depth analysis of lipid oxidation, due to limitations on sample amounts, there was no increased abundance of truncated oxidized PCs in the mass range *m/z* 590–670 [22].

4. Discussion

Lipidomic analysis of tracheal aspirate samples confirmed that the novel nebulization device successfully delivered Alveofact to the lungs of patients in the treated group, shown by the increased proportion of phospholipids characteristic of Alveofact in tracheal aspirates between $T = 8$ h and $T = 72$ h compared with samples at $T = 0$ h (Fig. 2A and B). This is the first detailed analysis of the phospholipid compositional changes after administration of a therapeutic dose exogenous surfactant to any patient group; it confirms that the nebulization previously reported in the ventilated pig model [13] is highly effective in the clinical setting. This was a pragmatic study which sampled tracheal aspirates to minimise health care-associated infections and patient decompensation during frequent bronchoscopy. But nevertheless, tracheal aspirates have

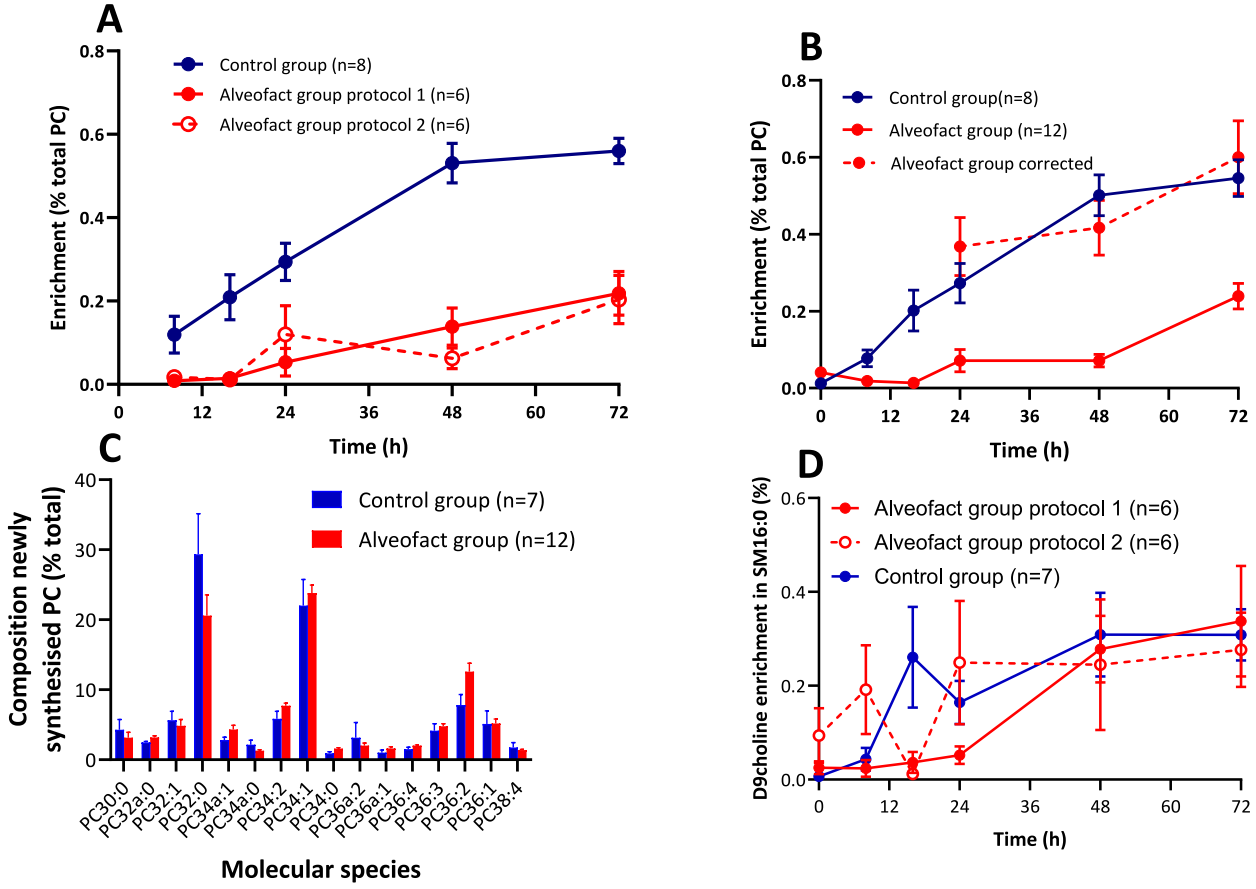

Fig. 5. Incorporation of *methyl*-D_9choline into tracheal aspirate phosphatidylcholine (panels A, B and C) and sphingomyelin (panel D). **A** *Methyl*-D_9choline enrichment in PC for the control group, Alveofact group protocol 1 and Alveofact group protocol 2; **B**. *Methyl*-D_9choline enrichment in PC for the same patient groups after correction for calculated endogenous lipid concentration; **C** Fractional composition of newly synthesised PC at $T = 72$ h between the control and Alveofact-treated groups; **D** *Methyl*-D_9choline enrichment in SM for the control group, Alveofact group protocol 1and Alveofact group protocol 2.

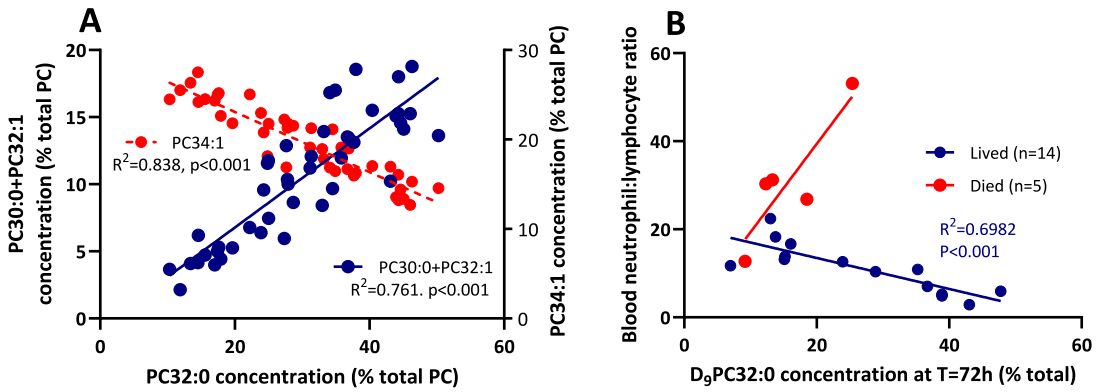

Fig. 6. **A** Correlations of PC species in TA samples from control subjects at all time points. PC30:0 and PC32:1 are characteristic of surfactant and track with PC32:0 while PC34:1 is more characteristic of cell membranes, suggesting total PC in TA samples is a combination of surfactant and cell derived PC; **B** The blood neutrophil to lymphocyte ratio at T = 72 h was negatively correlated with the fractional synthesis of D_9PC32:0 in all subjects who survived, an association that was lost in the subjects who died within 28 days.

been used previously in healthy volunteers and in ARDS patients to characterise surfactant metabolism [15,23]. One striking observation was the very high fractional concentration of PS at T = 0 h for all cohorts, illustrated by the comparison of negative ionisation scans and Fig. 2A and B, which were supressed initially after Alveofact nebulisation but substantially recovered by $T = 72$ h. It is possible that this high concentration of PS may contribute to the formation of microthrombi in the pulmonary capillary bed [21].

The devised novel methodology to estimate turnover based on comparing the different lipid profiles of Alveofact and tracheal aspirate samples was analogous to the lecithin:sphingomyelin ratio developed as a measure of lung immaturity in preterm infants [24]. This estimate of surfactant turnover rested on the assumption that the composition of endogenous phospholipid did not change over 72 h for patients in the treatment group but was diluted by the exogenous surfactant. This assumption is supported both by the minimal change in phospholipid composition in patients in the control group over this time (Fig. 2G) and by the substantial recovery of the original aspirate lipid composition at T = 72 h (Fig. 2E and F) in the treated groups. SM16:0, was chosen as the marker of endogenous lipid as it could be quantified reliably even in the most dilute samples.

Importantly, while the index of surfactant turnover was not a direct measure of exogenous surfactant concentration, as the upper value is set by the concentration of SM16:0 in Alveofact, it did enable kinetic modelling for estimating half-life and turnover for subjects recruited under protocol 1 (Fig. 3 and Supplementary Table 2). While the estimated half-life varied considerably between patients, this analysis indicated a rapid removal of exogenous surfactant from the airways and potentially the alveolus, such that little material remained at T = 72 h. This conclusion broadly agrees with the one other report of surfactant kinetics in ARDS patients, which followed the loss of a tracer amount of surfactant labelled with added ^{13}C-palmitate DPPC [23]. The indirect calculation of Alveofact half-life for patients in protocol 2 supports this rapid turnover of exogenous surfactant. Understandably, there are no comparative reports of the kinetics of therapeutic surfactant doses in healthy adult volunteers or in patients ventilated for non-respiratory reasons. The increased fractional synthesis of disaturated PC (DSPC) from deuterated water in ARDS patients compared with controls [25] is consistent with a faster catabolism of DSPC in the patient group. This rapid removal of exogenous surfactant may be one contributor to the failure of clinical trials of surfactant therapy in ARDS, in addition to the heterogeneity of the patient population and multiple initiating factors.

While our study did not address mechanisms of exogenous surfactant catabolism, the constant low concentration of LysoPC (Supplementary Fig. 3) provided no evidence for increased PC hydrolysis by $sPLA_2$ despite reports of increased enzyme activity in lung fluid from ARDS patients [26]. The most likely routes for loss of administered surfactant are uptake by lung parenchyma or hydrolysis by inflammatory cells. In addition, the SARS-COV-2 virus may lead to surfactant inhibition by interaction with the S2 subunit of the spike protein [28].

The maximal enrichment of *methyl*-D_9-choline incorporation into total PC in the control group (0.56 ± 0.08%, Fig. 4A) was lower than previously reported (0.90 ± 0.2%), but this may have been in part due to the lower dose of infused *methyl*-D_9-choline of 3.0 vs 3.6 mg/kg body weight (17). In addition, the maximum dose was 300 mg and two patients had an actual body weight of >100 kg. Dilution of endogenous lipid by Alveofact in the treated group complicated the enrichment analysis, but correction for this dilution indicated no significant effect of the exogenous surfactant on endogenous PC synthesis (Fig. 4B) in agreement with our previous analysis of lung PC synthesis in surfactant-treated mice [27].

An indication of the relative synthesis of surfactant compared with cellular PC was provided by the percentage distribution of label incorporation into individual molecular species. This distribution was calculated at $T = 72$ h, as acyl remodelling processes are essentially complete by this time [15,27]. The lack of effect of Alveofact administration on this incorporation pattern at T = 72 h suggested there was minimal effect of exogenous surfactant on the specificity of endogenous PC synthesis (Fig. 4C). However, as SM is not a significant component of surfactant, the incorporation of label into SM (Fig. 4D) provided strong evidence that a proportion of tracheal aspirate PC was synthesised by cells other than AT-II cells, most probably inflammatory or bronchial epithelial cells.

A number of observations support the concept that the phospholipids in these tracheal aspirate samples were derived from both surfactant and non-surfactant sources. The positive correlation of PC30:0 and PC32:1 with PC32:0 in the control group (Fig. 5A) is consistent with the reported co-ordinated specificity of their packaging PC into lamellar bodies in ATII cells [22]. While large changes to diet can modify mouse surfactant phospholipid [29], the extent of such changes is much smaller than those reported here. The corresponding inverse correlation of PC32:0 with PC34:1 might be due to two reasons. First, PC34:1 is associated with inflammatory cellular membrane phospholipids and increased inflammation is associated with reduced relative concentration of surfactant specific PC32:0. Second, PC34:1 and other unsaturated species are used during acyl-remodelling of surfactant PC to generate disaturated PC32:0 [1,2] [30,31]and may therefore have more rapid kinetics. To explore this further, we analysed surfactant synthesis by measuring the fractional composition of *methyl*-D_9 choline labelled PC32:0 at 72 h for all patients and correlated this with the plasma neutrophil to lymphocyte ratio (Fig. 5B). Patients who survived had a lower neutrophil to lymphocyte ratio which was associated with higher

fractional synthesis of PC 32:0, suggesting that the degree of inflammation may adversely contribute to surfactant synthesis. In common with other reported studies in COVID-19 infection [32], the blood neutrophil to lymphocyte ratio at $T = 0$ h was predictive of mortality within 28 days.

In conclusion, this is the first study to evaluate endogenous surfactant metabolism and exogenous surfactant pharmacokinetics in patients with COVID-19. The lipidomic results presented here demonstrate that breath-synchronized nebulization is an effective approach for the delivery of exogenous surfactant to mechanically ventilated patients. Our results suggest that exogenous surfactant does not enhance, inhibit or provide substrate for endogenous surfactant synthesis. The rapid disappearance of administered surfactant has direct implications for the design of clinical trials of surfactant therapy, not only for COVID-19 patients but also for other ARDS patients. While most adult ARDS studies demonstrated that surfactant supplementation transiently improved oxygenation [10], this was not sustained and our study clarifies one contributory factor behind these negative clinical trials. The results from this study support the hypothesis that pulmonary surfactant deficiency may play a role in critically ill patients receiving mechanical ventilation for severe COVID-19 infection. This study highlights several factors that need to be addressed in any future trials of surfactant therapy in ARDS, including choice of surfactant preparation, timing of administration in the disease process, and frequency and concentration of delivered doses.

CRediT authorship contribution statement

Anthony D. Postle: Writing – review & editing, Writing – original draft, Supervision, Resources, Methodology, Investigation, Funding acquisition, Formal analysis, Conceptualization. **Howard W. Clark:** Writing – review & editing, Writing – original draft, Investigation, Conceptualization. **James Fink:** Writing – review & editing, Writing – original draft, Resources, Methodology, Conceptualization. **Jens Madsen:** Writing – review & editing, Writing – original draft, Supervision, Project administration, Conceptualization. **Grielof Koster:** Writing – review & editing, Software, Methodology, Formal analysis. **Madhuriben Panchal:** Writing – review & editing, Investigation, Formal analysis. **Lewis Matthews:** Writing – review & editing, Investigation. **Lee Berry:** Writing – review & editing, Investigation. **Ratko Djukanovic:** Writing – review & editing, Funding acquisition, Conceptualization. **David Brealey:** Writing – review & editing, Project administration, Investigation, Conceptualization. **Michael P.W. Grocott:** Writing – review & editing, Writing – original draft, Project administration, Investigation, Funding acquisition, Conceptualization. **Ahilanandan Dushianthan:** Writing – review & editing, Writing – original draft, Supervision, Project administration, Investigation, Funding acquisition, Conceptualization.

Declaration of competing interest

The authors declare the following financial interests/personal relationships which may be considered as potential competing interests: Professor A.D. Postle reports financial support was provided by Bill & Melinda Gates Foundation. Professor H.W. Clark reports financial support was provided by NIHR University College London Hospitals Biomedical Research Centre. Professor M.P.H. Grocott reports financial support was provided by NIHR Southampton Biomedical Research Centre. If there are other authors, they declare that they have no known competing financial interests or personal relationships that could have appeared to influence the work reported in this paper.

Acknowledgments

We are grateful to the Bill and Melinda Gates Foundation for funding this study, to all the nursing and clinical staff in the Intensive Care Units at University Southampton Hospital and University College London Hospital, and to the members of the Patient Participation Panel. We also thank the TSC and DSMB committee members. The research was supported by researchers at the NIHR Southampton Biomedical Research Centre and the NIHR University College London Hospitals Biomedical Research Centre.

Appendix A. Supplementary data

Supplementary data to this article can be found online at https://doi.org/10.1016/j.bbalip.2026.159731.

Data availability

Data will be made available on request.

References

[1] M. Carcaterra, C. Caruso, Alveolar epithelial cell type II as main target of SARS-CoV-2 virus and COVID-19 development via NF-kb pathway deregulation: a physio-pathological theory, Med. Hypotheses 146 (2021) 110412.
[2] M. Hoffmann, H. Kleine-Weber, S. Schroeder, N. Kruger, T. Herrler, S. Erichsen, T. S. Schiergens, G. Herrler, N.H. Wu, A. Nitsche, M.A. Muller, C. Drosten, S. Pohlmann, SARS-CoV-2 cell entry depends on ACE2 and TMPRSS2 and is blocked by a clinically proven protease inhibitor, Cell 181 (2020) 271–280.
[3] L. Carsana, A. Sonzogni, A. Nasr, R.S. Rossi, A. Pellegrinelli, P. Zerbi, R. Rech, R. Colombo, S. Antinori, M. Corbellino, M. Galli, E. Catena, A. Tosoni, A. Gianatti, M. Nebuloni, Pulmonary post-mortem findings in a series of COVID-19 cases from northern Italy: a two-Centre descriptive study, Lancet Infect. Dis. 20 (2020) 1135–1140.
[4] J.J. Batenburg, Surfactant phospholipids: synthesis and storage, Am. J. Phys. Lung Cell. Mol. Phys. 262 (1992) L367–L385.
[5] A. Günther, C. Siebert, R. Schmidt, S. Ziegler, F. Grimminger, M. Yabut, B. Temmesfeld, D. Walmrath, H. Morr, W. Seeger, Surfactant alterations in severe pneumonia, acute respiratory distress syndrome, and cardiogenic lung edema, Am. J. Respir. Crit. Care Med. 153 (1996) 176–184.
[6] R.J. Mason, Thoughts on the alveolar phase of COVID-19, Am. J. Phys. Lung Cell. Mol. Phys. 319 (2020) L115–L120.
[7] S. Piva, R.M. DiBlasi, A.E. Slee, A.H. Jobe, A.M. Roccaro, M. Filippini, N. Latronico, M. Bertoni, J.C. Marshall, M.A. Portman, Surfactant therapy for COVID-19 related ARDS: a retrospective case-control pilot study, Respir. Res. 22 (2021) 20.
[8] K.H. Briones-Claudett, M.H. Briones-Claudett, C.K. Bajana Huilcapi, O.E. Tripul Villamar, R. Ochoa Vasquez, C.D.R. Rivera Salas, K.H. Briones-Zamora, J. Benites Solis, D.C. Briones-Marquez, A.X. Freire, M. Grunauer, Surfactant therapy using vibrating-mesh nebulizers in adults with COVID-19-induced ARDS: a case series, SAGE Open Med. Case Rep. 12 (2024) 2050313X241236313.
[9] A. Dushianthan, H.W. Clark, D. Brealey, D. Pratt, J.B. Fink, J. Madsen, H. Moyses, L. Matthews, T. Hussell, R. Djukanovic, M. Feelisch, A.D. Postle, M.P.W. Grocott, A randomized controlled trial of nebulized surfactant for the treatment of severe COVID-19 in adults (COVSurf trial), Sci. Rep. 13 (2023) 20946.
[10] S.S. Meng, W. Chang, Z.H. Lu, J.F. Xie, H.B. Qiu, Y. Yang, F.M. Guo, Effect of surfactant administration on outcomes of adult patients in acute respiratory distress syndrome: a meta-analysis of randomized controlled trials, BMC Pulm. Med. 19 (2019) 9.
[11] A. Dushianthan, R. Cusack, V. Goss, A.D. Postle, M.P. Grocott, Clinical review: Exogenous surfactant therapy for acute lung injury/acute respiratory distress syndrome–where do we go from here? Crit. Care 16 (2012) 238.
[12] A. Anzueto, R.P. Baughman, K.K. Guntupalli, J.G. Weg, H.P. Wiedemann, A. A. Raventos, F. Lemaire, W. Long, D.S. Zaccardelli, E.N. Pattishall, Aerosolized surfactant in adults with sepsis-induced acute respiratory distress syndrome. Exosurf acute respiratory distress syndrome Sepsis study group, N. Engl. J. Med. 334 (1996) 1417–1421.
[13] R.M. DiBlasi, M. Kajimoto, J.A. Poli, G. Deutsch, J. Pfeiffer, J. Zimmerman, D. N. Crotwell, P. Malone, J.B. Fink, C. Ringer, R. Uthamanthil, D. Ledee, M. A. Portman, Breath-synchronized nebulized surfactant in a porcine model of acute respiratory distress syndrome, Crit Care Explor 3 (2021) e0338.
[14] A. Dushianthan, H. Clark, J. Madsen, R. Mogg, L. Matthews, L. Berry, J.B. de la Serna, J. Batchelor, D. Brealey, T. Hussell, J. Porter, R. Djukanovic, M. Feelisch, A. Postle, M.P.W. Grocott, Nebulised surfactant for the treatment of severe COVID-19 in adults (COV-surf): a structured summary of a study protocol for a randomized controlled trial, Trials 21 (2020) 1014.
[15] A. Dushianthan, V. Goss, R. Cusack, M.P. Grocott, A.D. Postle, Phospholipid composition and kinetics in different endobronchial fractions from healthy volunteers, BMC Pulm. Med. 14 (2014) 10.
[16] K.C.W. Goss, V.M. Goss, J.P. Townsend, G. Koster, H.W. Clark, A.D. Postle, Postnatal adaptations of phosphatidylcholine metabolism in extremely preterm infants: implications for choline and PUFA metabolism, Am. J. Clin. Nutr. 112 (2020) 1438–1447.
[17] A. Dushianthan, V. Goss, R. Cusack, M.P. Grocott, A.D. Postle, Altered molecular specificity of surfactant phosphatidycholine synthesis in patients with acute respiratory distress syndrome, Respir. Res. 15 (2014) 128.

[18] M. Griese, P. Dietrich, D. Reinhardt, Pharmacokinetics of bovine surfactant in neonatal respiratory distress syndrome, Am. J. Respir. Crit. Care Med. 152 (1995) 1050–1054.
[19] M. Hammoud, N. Al-Kazmi, M. Alshemmiri, L. Thalib, V.T. Ranjani, L. V. Devarajan, H. Elsori, Randomized clinical trial comparing two natural surfactant preparations to treat respiratory distress syndrome, J. Matern. Fetal Neonatal Med. 15 (2004) 167–175.
[20] A.D. Postle, H.W. Clark, J. Fink, J. Madsen, G. Koster, M. Panchal, R. Djukanovic, D. Brealey, M.P.W. Grocott, A. Dushianthan, Rapid phospholipid turnover after surfactant nebulization in severe COVID-19 infection: a randomized clinical trial, Am. J. Respir. Crit. Care Med. 205 (2022) 471–473.
[21] C. Wang, C. Yu, V.A. Novakovic, R. Xie, J. Shi, Circulating microparticles in the pathogenesis and early anticoagulation of thrombosis in COVID-19 with kidney injury, Front. Cell Dev. Biol. 9 (2021) 784505.
[22] V. Goss, A.N. Hunt, A.D. Postle, Regulation of lung surfactant phospholipid synthesis and metabolism, Biochim. Biophys. Acta 1831 (2013) 448–458.
[23] P.E. Cogo, G.M. Toffolo, C. Ori, A. Vianello, M. Chierici, A. Gucciardi, C. Cobelli, A. Baritussio, V.P. Carnielli, Surfactant disaturated-phosphatidylcholine kinetics in acute respiratory distress syndrome by stable isotopes and a two compartment model, Respir. Res. 8 (2007) 13.
[24] J.F. Roux, J. Nakamura, E. Brown, A.Y. Sweet, L. Gluck, The lecithin-sphingomyelin ratio of amniotic fluid: an index of fetal lung maturity? Pediatrics 49 (1972) 464–467.
[25] M. Simonato, A. Baritussio, C. Ori, L. Vedovelli, S. Rossi, M.L. Dalla, S. Rizzi, V. P. Carnielli, P.E. Cogo, Disaturated-phosphatidylcholine and surfactant protein-B turnover in human acute lung injury and in control patients, Respir. Res. 12 (2011) 36.
[26] L. Arbibe, K. Koumanov, D. Vial, C. Rougeot, G. Faure, N. Havet, S. Longacre, B. B. Vargaftig, G. Bereziat, D.R. Voelker, C. Wolf, L. Touqui, Generation of lyso-phospholipids from surfactant in acute lung injury is mediated by type-II phospholipase A2 and inhibited by a direct surfactant protein a-phospholipase A2 protein interaction, J. Clin. Invest. 102 (1998) 1152–1160.
[27] J. Madsen, M.H. Panchal, R.A. Mackay, M. Echaide, G. Koster, G. Aquino, N. Pelizzi, J. Perez-Gil, F. Salomone, H.W. Clark, A.D. Postle, Metabolism of a synthetic compared with a natural therapeutic pulmonary surfactant in adult mice, J. Lipid Res. 59 (2018) 1880–1892.
[28] G. Li, B. Sun, Y.Y. Zuo, Biohysical mechanisms of SARS-COV-2-induced surfactant inhibition, Biophys. J. 123 (2025) 3733–3744.
[29] J. Schipke, D. Jutte, C. Brandenberger, C. Autilio, J. Perez-Gil, W. Bernhard, M. Ochs, C. Muhlfeld, Dietary carbohydrates and fat induce distinct surfactant alterations in mice, Am. J. Respir. Cell Mol. Biol. 64 (2021) 379–390.
[30] A.D. Postle, N.G. Henderson, G. Koster, H.W. Clark, A.N. Hunt, Analysis of lung surfactant phosphatidylcholine metabolism in transgenic mice using stable isotopes, Chem. Phys. Lipids 164 (2011) 549–555.
[31] J.P. Bridges, M. Ikegami, L.L. Brilli, X. Chen, R.J. Mason, J.M. Shannon, LPCAT1 regulates surfactant phospholipid synthesis and is required for transitioning to air breathing in mice, J. Clin. Invest. 120 (2010) 1736–1748.
[32] L. Turgunova, I. Mekhantseva, L. Akhmaltdinova, M. Kostinov, Z. Zhumadilova, A. Turmukhambetova, Association of sTREM-1 and neutrophil-to-lymphocyte ratio as prognostic markers in COVID-19 short- and long-yerm mortality, J. Inflamm. Res. 16 (2023) 5807–5817.